

Dartmouth College

Dartmouth Digital Commons

Dartmouth Scholarship

Faculty Work

5-27-2003

Vam10p Defines a Sec18p-Independent step of Priming that Allows Yeast Vacuole Tethering

Masashi Kato
Dartmouth College

William Wickner
Dartmouth College

Follow this and additional works at: <https://digitalcommons.dartmouth.edu/facoa>



Part of the [Medical Biochemistry Commons](#)

Dartmouth Digital Commons Citation

Kato, Masashi and Wickner, William, "Vam10p Defines a Sec18p-Independent step of Priming that Allows Yeast Vacuole Tethering" (2003). *Dartmouth Scholarship*. 1408.
<https://digitalcommons.dartmouth.edu/facoa/1408>

This Article is brought to you for free and open access by the Faculty Work at Dartmouth Digital Commons. It has been accepted for inclusion in Dartmouth Scholarship by an authorized administrator of Dartmouth Digital Commons. For more information, please contact dartmouthdigitalcommons@groups.dartmouth.edu.

Vam10p defines a Sec18p-independent step of priming that allows yeast vacuole tethering

Masashi Kato and William Wickner*

Department of Biochemistry, Dartmouth Medical School, 7200 Vail Building, Hanover, NH 03755-3844

Contributed by William Wickner, April 11, 2003

YOR068c, termed VAM10 (altered vacuole morphology), lies within the VPS5 gene on the opposite DNA strand. VAM10 deletion causes vacuole fragmentation *in vivo*. The *in vitro* fusion of purified yeast vacuoles is stimulated by recombinant Vam10p and blocked by antibody to Vam10p. Vam10p acts early in the priming stage of fusion, independent of Sec18p. After priming, recombinant Vam10p will not stimulate fusion and anti-Vam10p antibodies will not inhibit; Vam10p provides a functional marker for this Sec18p-independent priming step. Pure Vam10p restores normal, Ypt7p-dependent tethering to vacuoles from a *vam10Δ* strain.

Membrane fusion is regulated and catalyzed by similar factors for each organelle and organism (1). These include Rab/Ypt and Rho family GTPases, their nucleotide exchange and GTPase-activating proteins, other tethering proteins and effectors, soluble *N*-ethylmaleimide-sensitive fusion proteins (SNAREs), SNARE-associated proteins such as the Munc18/Sec1 family, chaperones, phosphoinositides, sterols, actin, calcium, and calcium-binding proteins. The complexity of regulated trafficking and membrane fusion suggests that additional factors remain to be discovered.

We study membrane fusion mechanisms with yeast vacuoles (2). Homotypic vacuole fusion occurs in three stages: (i) priming, which precedes vacuole association, (ii) tethering and docking, in which vacuoles form clusters, and (iii) fusion, the mixing of the bilayers and luminal contents. Sec18p ATPase drives Sec17p release during priming (3), disassembling the cis-SNARE complex. In addition to Sec18p action, lipid synthesis (4) and acylation of Vac8p (5) occur during priming. Docking occurs in three subreactions: tethering, vertex ring assembly, and trans-SNARE pairing. Tethering is mediated by the Ypt7p GTPase (6). Ypt7p is enriched at a "vertex ring" microdomain that surrounds the apposed membranes of tethered vacuoles (7). Conversion of Ypt7p to its GTP-bound form and remodeling of vacuolar actin allow the SNAREs, the HOPS/VPS class C effector complex, and actin to assemble into the vertex ring (7, 8). The assembled ring allows trans-SNARE pairing. Fusion is initiated by a flux of calcium from the vacuole lumen (9).

A genomic approach has identified genes involved in vacuole fusion (10). We screened a commercially available yeast library of nonessential gene deletions for their vacuole morphology; deletion of a vacuole fusion gene causes fragmented vacuoles. Among the strains with abnormal vacuole morphology (*vam* phenotype; ref. 11) were 28 ORFs encoding proteins of unknown function.

We now report that one ORF, *YOR068c* (*VAM10*), catalyzes an early and novel stage of the priming subreaction, a stage that can proceed independently of Sec18p and ATP-mediated disassembly of the cis-SNARE complex. Vam10p acts during priming to permit vacuole tethering.

Methods

Yeast Strains. Strains BJ3505 and DKY6281 have been described (12). Deletions of *yor068c*, *ydr136w*, and *vps5* in BY4742 were purchased from Research Genetics (Huntsville, AL). Deletions of *pep4* or *pho8* were made in *vam10* (*yor068c*)Δ as described (9). *Yor068p* and *Ybr174p* were overexpressed in yeast strain Y258,

fused to GST-HisX6 at their NH₂ termini, and expressed from *GAL1* (ref. 13; a gift from M. Snyder, Yale University, New Haven, CT).

Proteins. Proteins tagged with C-terminal maltose binding protein (MBP) were expressed in *Escherichia coli* BL21(DE3) (Novagen) with pMAL-c2x (New England Biolabs) containing in-frame *EcoRI*-*XbaI* (*vam10*) or *EcoRI*-*BamHI* (*ydr136c*) PCR products. MBP-tagged full-length *Yor068p* and truncated *Ydr136p* (61 aa; from "FALPR" to "PPHGE") were purified by amylose affinity chromatography (New England Biolabs). Whole-cell lysates were prepared as described (14). IgG was prepared by Sephacryl S-200 HR gel filtration (Pharmacia) after isolation on protein A Sepharose CL-4B (Pharmacia). Vam10p antibody was affinity-purified on peptide crosslinked to Affi-Gel 10 (Bio-Rad).

Vacuole Fusion. Standard reactions contained 3 μg of each of frozen vacuoles from BJ3505 and DKY6281 in 30–35 μl of reaction buffer (10 mM Pipes-KOH, pH 6.8/200 mM sorbitol/125 mM NH₄Cl/5 mM MgCl₂/10 μM CoA/8 μg/ml IB2/1 mM Mg-ATP/40 mM creatine phosphate/0.5 mg/ml creatine kinase/6.6 ng/ml leupeptin/16.6 ng/ml pepstatin/16.6 μM *o*-phenanthroline/3.3 μM Pefabloc SC). After 90 min at 27°C, alkaline phosphatase was assayed (12).

Yeast Expression of Vam10p and Vps5p. The pRS316 vector, this vector bearing *VPS5* and *VAM10* (nucleotides 453367–456210) or bearing this fragment with a T-to-A mutation at residue 454213, abolishing *VAM10* expression by changing its initiator Met codon to a Lys codon while not changing the amino acyl residues encoded on the opposite strand (for *VPS5*), was transformed into wild-type, *vam10Δ*, or *vps5Δ* yeast. The latter deletion is the 3' end of the *VPS5* gene, shown in the unshaded box in Fig. 3A. To do this, the *VPS5* gene with its native promoter and terminator (and with a point mutation in the start codon of *VAM10*, where indicated) was amplified by PCR, using CCAAGCTTTTCGCGGCAGTCTTC and CCGCTCGAGGTTACACCAACAAAAGA with *HindIII* and *XhoI* sites. The point mutation was made by the QuikChange site-directed mutagenesis kit (Stratagene), using CCAAATACTTCAAAAAGCTTCTCTGGAAGAAGATCCGG and CCGGATCTTCTTCCAGAGAAGCTTTTTGAAGTATTTGG. The plasmid pRS316 (New England Biolabs) without insert or bearing the PCR product encoding both *VPS5* and *VAM10* or these genes with T454213A was transformed into BY4742, BY4742 bearing deletion of *vam10* (and the corresponding 5' region of the *vps5* genes), and BY4742 bearing deletion of nucleotides 454858–455796, the 3' region of *vps5*. Transformants were selected on SD-ura (Bio 101) and screened for integration by RT-PCR, using ATGGACTACGAGGATAATCT (5'-*VPS5*), CTAAAGATTGGTTTGGTAGAA (3'-*VPS5*), AAGTATTTGGTGAAGTGTTAG (5'-*VAM10*), and

Abbreviations: SNARE, soluble *N*-ethylmaleimide-sensitive fusion protein; YPD, yeast extract/peptone/dextrose.

*To whom correspondence should be addressed. E-mail: Bill.Wickner@Dartmouth.edu.

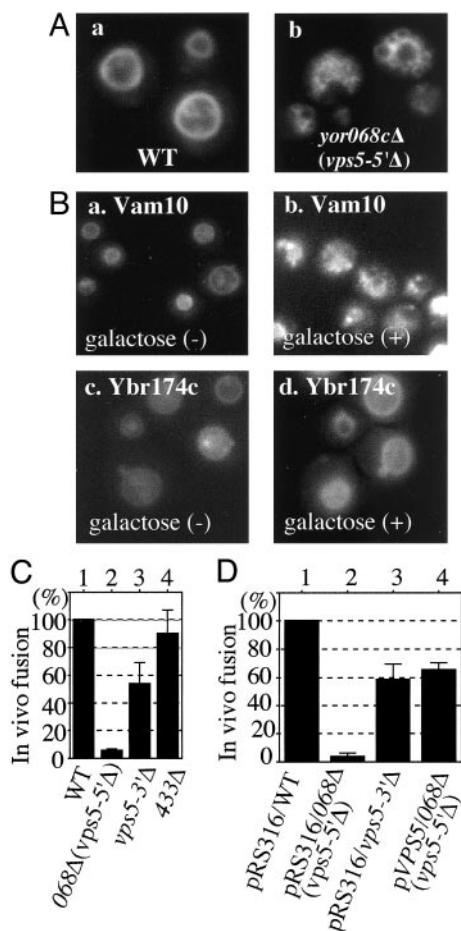


Fig. 1. Vacuole fusion *in vivo*. (A) Wild-type (WT) strain BY4742 (a) and *yor068*Δ (b) were grown in 0.2 ml of yeast extract/peptone/dextrose (YPD) in 15-ml culture tubes at 30°C. After 16 h, 0.4 ml of YPD with 5 μM FM4-64 (15) was added, incubation was continued for 4 h at 30°C, and cells were photographed (7). (B) Vacuole morphology before and after induction of Vam10p (a and b) and Ybr174c (c and d) by galactose. (C) Osmotic stress-induced vacuole fusion. WT strain BY4742 (lane 1) and *yor068*Δ (lane 2), *vps5-3'Δ* (lane 3), and *ydr433wΔ* strains were grown in 0.5 ml of YPD in 15-ml culture tubes at 30°C. After 16 h, 1 ml of YPD with 5 μM FM4-64 was added and incubation was continued at 30°C until OD₆₀₀ = 5 (4–5 h). Samples (400 μl) were centrifuged (6,000 × *g* for 30 sec) and cells were resuspended in 350 μl of water. After 3 min at 23°C, *in vivo* vacuole fusion events were counted for 4 min in eight fields (30 sec per field). The average and SD of five experiments are presented. (D) Vector pRS316-transformed WT strain BY4742 (lane 1) and *yor068*Δ (lane 2), *vps5*Δ (lane 3), and pVP55-transformed *yor068*Δ (lane 4) strains were grown in 0.5 ml of SD-ura medium and analyzed as above.

AATATCTACAAATGAAGAAAGAA (3'-*VAM10*), and by the presence or absence of a *HindIII* site (AAGCTT).

Results

Vacuoles are fragmented when *YOR068c* is deleted (Fig. 1A; ref. 10) or overexpressed from a plasmid under *GAL* regulation (Fig. 1B). Vacuoles normally fuse on exposure of cells to low osmolarity (16); these *in vivo* fusion events were counted during a 30-sec window 3 min after cells were transferred to hypoosmolar medium. Deletion of *YOR068c* prevented osmotic stress-induced vacuole fusion *in vivo* (Fig. 1C, lane 2).

In accord with these *in vivo* studies, the *YOR068c*-encoded protein (068p), fused to MBP, stimulates *in vitro* vacuole fusion. To assay fusion, we isolate vacuoles from two strains, one with normal proteases but lacking the PHO8 phosphatase, the other with a normal PHO8 gene but lacking luminal proteases and,

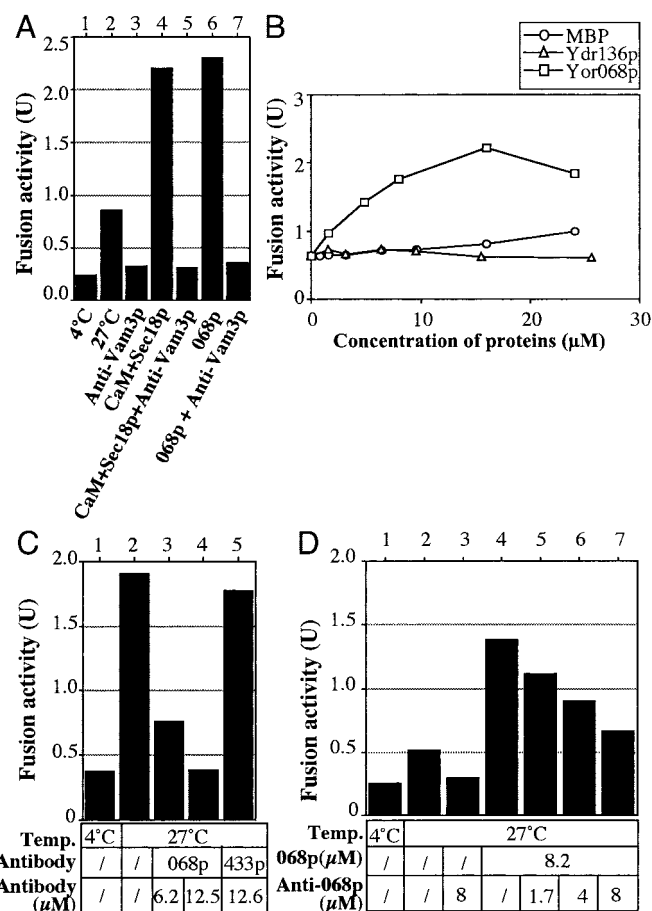


Fig. 2. *YOR068p* promotes vacuole fusion. (A) Fusion reactions with vacuoles from BJ3505 and DKY6281 were performed with anti-Vam3p antibody (1 μM), calmodulin (CaM; 20 μM), his₆-Sec18p (0.1 μM), or MBP-tagged Vam10p (Vam10p; 8 μM) as indicated. (B) Fusion reactions contained the indicated concentrations of MBP, Yor068p, or Ydr136p, each with an MBP tag. (C) Fusion reactions bore control buffer (lanes 1 and 2) or the indicated concentrations of anti-Vam10p (lanes 3 and 4) or anti-Ydr433p antibody. These IgG antibodies were purified as described (18). (D) Standard fusion reactions contained PS buffer (10 mM Pipes-KOH, pH 6.8/200 mM sorbitol; lanes 1 and 2) or the indicated concentrations of anti-Vam10p antibody (IgG fraction; lanes 3 and 5–7) and/or Vam10p (lanes 4–7).

thus, with catalytically inactive proPho8p. On fusion, proPho8p is cleaved to the mature active enzyme (12). Stimulated fusion (Fig. 2A, lane 2 vs. 6) was blocked by antibody to Vam3p (lane 7), showing that it is on the normal fusion pathway. MBP or other protein fusions with MBP did not stimulate (Fig. 2B). Other pure proteins, such as Sec18p and calmodulin, caused similar stimulation of fusion (Fig. 2A, lane 4; also see ref. 17), but combinations of these proteins with *YOR068p* did not enhance fusion (data not shown). Antibody to Vam10p (or Fab; data not shown) inhibited the fusion of purified vacuoles (Fig. 2C, lanes 2–4). Inhibition was dose dependent and was reversed by the addition of recombinant Vam10p (Fig. 2D). Further studies also point to a direct role for *YOR068c* in vacuole fusion, and, therefore, we name this protein Vam10p (11).

The *VAM10* gene is in a cluster of membrane-trafficking genes (Fig. 3A). It lies within *VPS5*, encoded on the opposite DNA strand. Genetic studies distinguish the functions of *VAM10* and *VPS5*. Deletion of the *VAM10* gene causes a large deletion in the 5' domain of *VPS5*, which we term *vps5-5'Δ*, whereas deletion from 454858 to 455796 in the 3' domain of *VPS5* (unshaded *VPS5-3'* box; Fig. 3A) leaves the *VAM10* gene intact. Yeast with

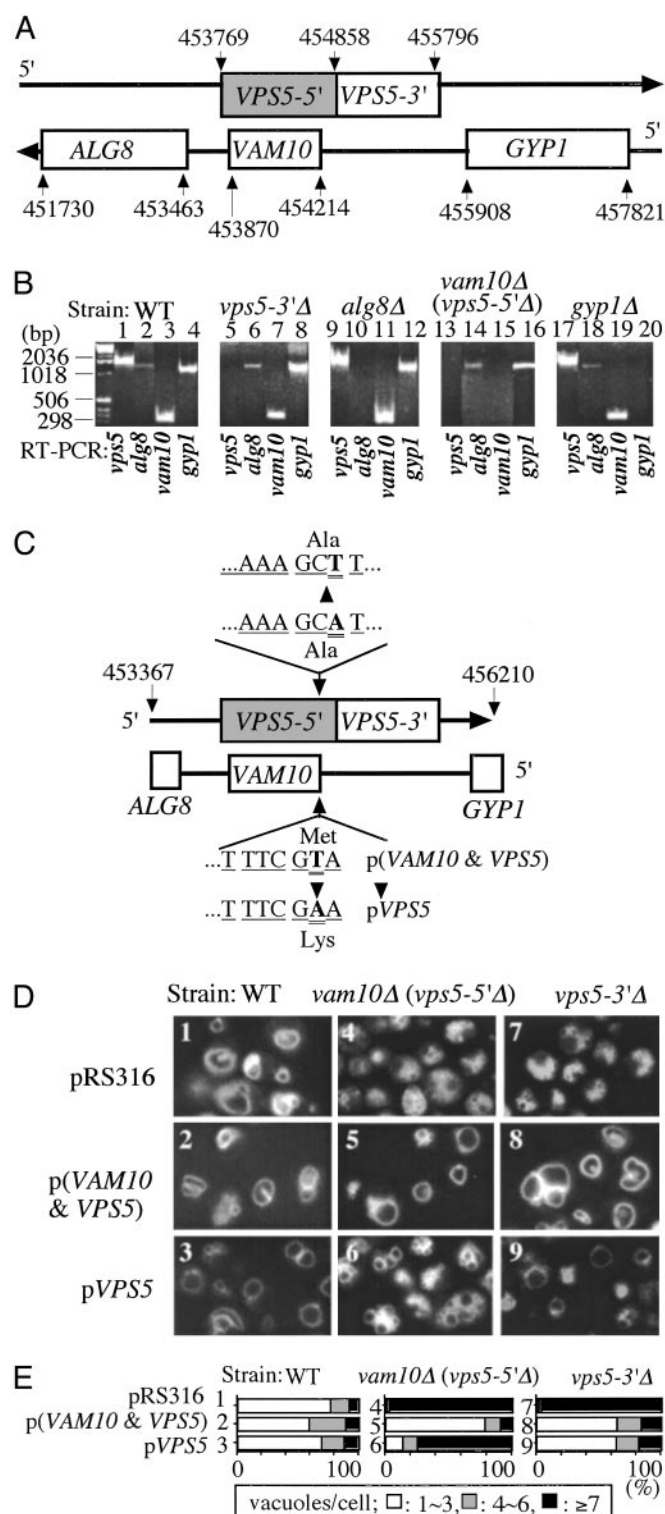


Fig. 3. Relationship of *VPS5* and *VAM10*. (A) Map of the *ALG8*, *VAM10*, *VPS5*, *GYP1* region. The *VPS5* gene encompasses 2,028 bp (shaded plus open boxes in the figure), from 453769 to 455796 (19, 20), although only residues 454858–455796 were removed in the *vps5Δ* strain. The *VAM10* gene lies within the *VPS5* gene on the opposite strand. (B) Levels of mRNA from *ALG8*, *VAM10*, *VPS5*, and *GYP1* genes in BY4742 and BY4742 mutants bearing deletions, which were assayed by RT-PCR by using the oligonucleotides listed in C for *VPS5* and *VAM10* and GGCTCCATTGTCGCCG (5'-*ALG8*), TCACTGCCATAGTA-ATTCGT (3'-*ALG8*), TACACAGGCCTGTTGTTTG (5'-*GYP1*), and TTACAGCCAGT-GCGACGT (3'-*GYP1*). RNA preparation used RNase-free DNase I and TRIzol (Invitrogen). Samples also were analyzed without the RT step to confirm the

each of these deletions, as well as the isogenic wild type, was purchased. RT-PCR analysis shows that each deletion ablates the corresponding transcript (Fig. 3B). Deletion of *VAM10* also abolishes the production of full-length *VPS5* transcript (Fig. 3B, lane 13), whereas deletion of the 3' half of *VPS5* allows *VAM10* transcription (lane 7). Plasmid p(*VAM10* and *VPS5*) was prepared (Fig. 3C) that expresses both the normal *VAM10* and *VPS5* genes. A derivative plasmid with a T454213A mutation abolishes the start codon for *VAM10* but leaves the normal amino acid sequence of Vps5p (Fig. 3C); this plasmid is termed p*VPS5*. Control vector, the vector expressing Vam10p and Vps5p, and the vector expressing Vps5p alone were transformed into wild-type BY4742 or into this strain deleted for *VAM10* (and, hence, the 5' domain of *VPS5*) or for the 3' domain of *VPS5*. Vacuole morphology was examined in each of these strains (Fig. 3D). Whereas BY4742 wild-type yeast have one to three vacuoles in most cells (Fig. 3D, 1), *vam10Δ* (*vps5-5'Δ*) or *vps5-3'Δ* causes fragmentation (Fig. 3D, 4 and 7). Coexpression of Vps5p and Vam10p from p(*VAM10* and *VPS5*) cures the vacuole fragmentation in *vam10Δ* (*vps5-5'Δ*) or *vps5-3'Δ* backgrounds (Fig. 3D5 and D8). However, expression of Vps5p alone cures the *vps5-3'Δ* phenotype (Fig. 3D9) but does not cure the *vam10Δ* (*vps5-5'Δ*) phenotype (Fig. 3D6), establishing a distinct role for Vam10p in vacuole morphology. Quantitation of vacuole number in cells from multiple microscopy fields (Fig. 3E) confirms these visual impressions. Thus, Vam10p and Vps5p each are needed for normal vacuole morphology.

With these strains, we returned to the *in vivo* assay of osmolarity-induced fusion to distinguish the roles of Vam10p and Vps5p. Vacuole fusion (Fig. 1D, lane 1) was abolished by the deletion of *VAM10* and, hence, truncation of *VPS5* (lane 2). Intermediate fusion rates were seen when only one of the *VPS5* or *VAM10* genes was expressed (lanes 3 and 4). Thus, both *VAM10* and *VPS5* are required for normal vacuole fusion. Further studies may determine whether Vps5p has a direct role in vacuole fusion or only governs vacuole morphology through its role in biosynthetic protein delivery to the vacuole.

Vam10p is needed on at least one vacuole in a fusion pair (Fig. 4A). Our *in vitro* fusion assay was performed with vacuoles from *pep4Δ* and *pho8Δ* strains that were *vam10Δ* (*vps5-5'Δ*), with expression of Vps5p, or both Vps5p and Vam10p, from plasmids. The absence of Vam10p from even one of the two vacuoles inhibited fusion (lanes 4 and 6), but fusion was abolished by the complete absence of Vam10p (lane 8). This was not due to a deficiency in Pep4p or Pho8p (Fig. 4B). Many other proteins known to be required for fusion also were present at normal levels in the absence of Vam10p (Fig. 4C). Carboxypeptidase Y was present at normal levels in vacuoles from cells lacking Vam10p, showing that *VAM10* is not a *VPS* gene. Strikingly, Sec18p, the HOPS subunits Vps39p and Vps41p, and actin were enriched on vacuoles lacking Vam10p (Fig. 4C). Each of these proteins is involved in early stages of the reaction, suggesting that Vam10p may function early in the fusion pathway.

To determine where Vam10p acts, we analyzed the kinetics with which vacuoles acquired resistance to antibodies to Vam10p. Fusion reaction aliquots either were placed on ice,

RNA origins of the RT-PCR products (data not shown). (C) Plasmids for gene expression were prepared as described in *Methods*. (D) Vacuole morphology was examined in WT, *vam10Δ* (*vps5-5'Δ*), and *vps5-3'Δ* strains bearing the control plasmid (pRS316), p(*VAM10* and *VPS5*), or p*VPS5* prepared as in B above, which were grown in 0.5 ml of 5D-ura medium in 15-ml tubes at 30°C. After 16 h, 1 ml of YPD with 5 μM FM4-64 was added, incubation was continued for 4 h, and vacuole morphology was examined. Pictures of multiple fields were taken for each condition. (E) For each of the strains shown in D, the percentage that have one to three, four to six, or more than seven vacuoles was scored for 120–160 cells.

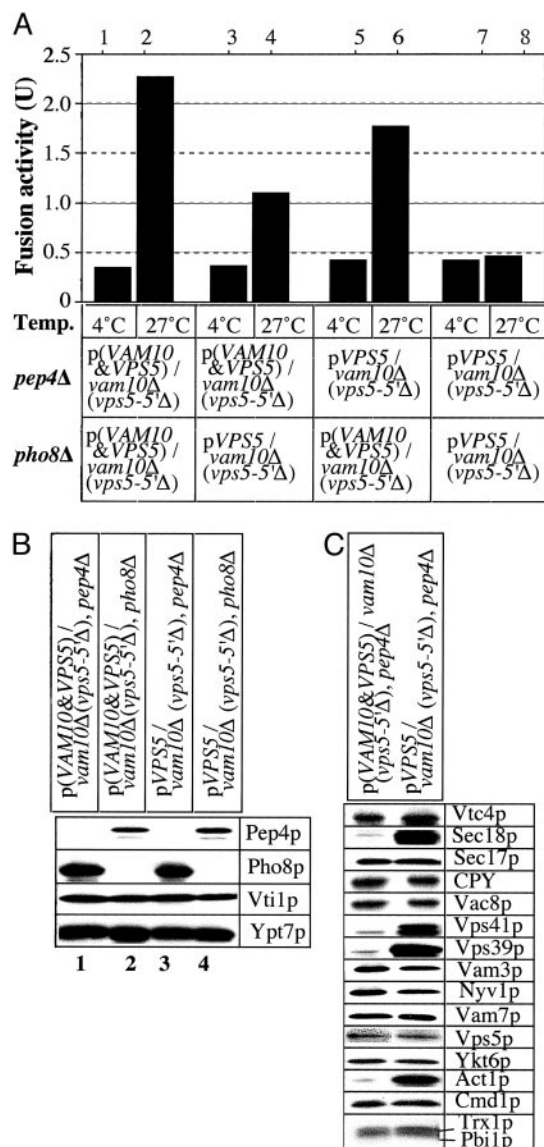


Fig. 4. Fusion activity and protein composition of vacuoles from *vam10Δ* cells. (A) Standard fusion assays were performed with vacuoles from *VAM10*, *pep4Δ*; *VAM10*, *pho8Δ*; *vam10Δ*, *pep4Δ*; and *vam10Δ*, *pho8Δ* strains. (B and C) Vacuoles (6 μg) from each indicated strain were analyzed by immunoblotting.

mixed with buffer, or mixed with antibody to Vam10p, to Sec17p or Sec18p (which catalyze priming), or to Vam3p to inhibit docking (Fig. 5A). All incubations were continued to 90 min, when samples were assayed for active, mature Pho8p. Each inhibitor completely blocked fusion when added at the start of the incubation. The reaction rapidly became resistant to antibody to Sec17p or Sec18p, reflecting their early priming role. Resistance to anti-Vam10p (Fig. 5A) occurred in parallel with resistance to antibody to Sec17p or Sec18p, suggesting that Vam10p functions exclusively during priming. Fusion reactions also were performed with the addition of either recombinant Vam10p or buffer at various times. Fusion was stimulated when Vam10p was added at early reaction times but not after 15 min of incubation (Fig. 5B). Clearly, Vam10p only acts early in the reaction.

Are Vam10p and Sec17/18p activities related? Anti-Sec18p blockade is reversed by the addition of recombinant Sec18p (3).

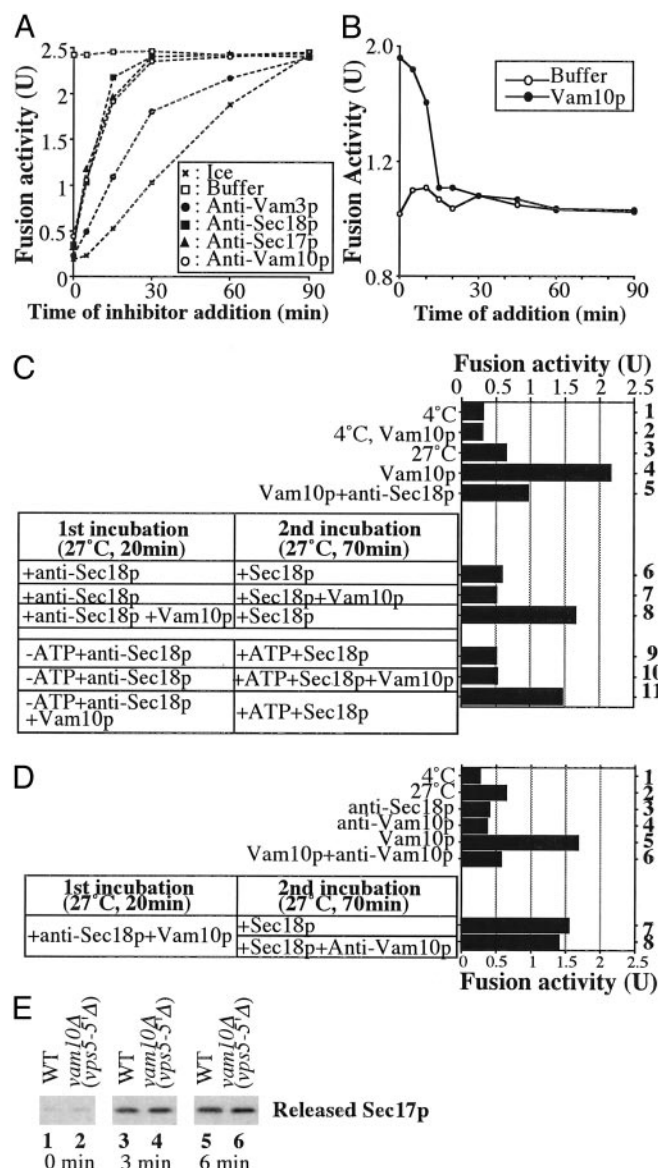


Fig. 5. Vam10p acts at a novel priming stage. (A) Reactions (1,350 μl) had BJ3505 and DKY6281 vacuoles and 4 μM Vam10p. Aliquots (30 μl) were placed on ice or added to inhibitors [anti-Sec17p (final concentration, 1 μM), anti-Sec18p (1 μM), anti-Vam3p (1 μM), and anti-Vam10p (4.9 μM)] at the indicated times. After 90 min, alkaline phosphatase was measured. (B) Aliquots (30 μl) were removed from a standard fusion reaction (300 μl) and added to PS buffer or to Vam10p (final concentration, 8 μM) at the indicated times. After 90 min, phosphatase was assayed. (C) Standard fusion reactions contained 8 μM Vam10p (lanes 2, 4, and 5) and 0.33 μM anti-Sec18p antibody (lane 5) at 4°C (lanes 1 and 2) or 27°C (lanes 3–5). Certain reactions were started with 0.33 μM anti-Sec18p in the presence (lanes 8 and 11) or absence (lanes 6, 7, 9, and 10) of 8 μM Vam10p under plus (lanes 6–8) or minus (lanes 9–11) ATP conditions. After 20 min at 27°C, samples received 8 μM Vam10p (lanes 7 and 10), ATP (lanes 9–11), or PS buffer. After further incubation for 70 min at 27°C, phosphatase was measured. (D) Fusion reactions contained 4 μM Vam10p (lanes 5 and 6), 8 μM anti-Vam10p (lanes 4 and 6), or 0.33 μM anti-Sec18p (lane 3) at 4°C (lane 1) or 27°C (lanes 2–6). Reactions were started with 0.33 μM anti-Sec18p with 4 μM Vam10p (lanes 7 and 8). After 20 min at 27°C, samples received 0.16 μM Sec18p with (lane 7) or without (lane 8) 8 μM anti-Vam10p. After 70 min at 27°C, phosphatase was measured. (E) After incubating fusion reactions with vacuoles from wild-type or *yor068Δ* strains with 0.018 μM Sec18p for the indicated times, vacuoles were removed by centrifugation and supernatants were analyzed by immunoblotting with anti-Sec17p (3).

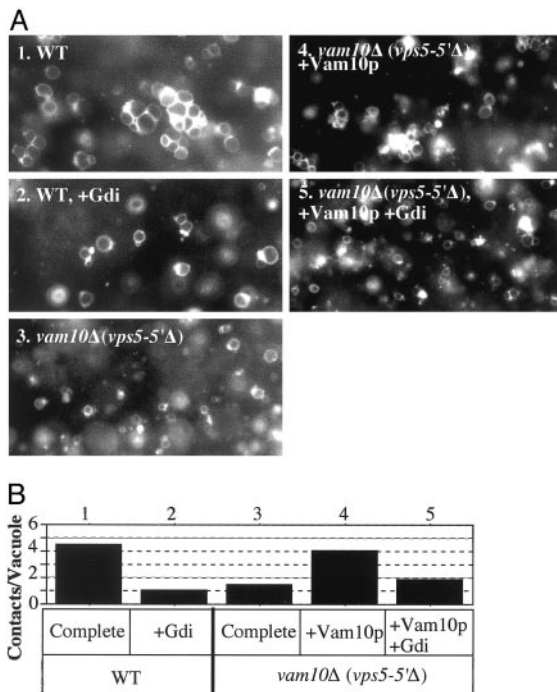


Fig. 6. Vam10p supports tethering. (A) Docking assays (7) had 6 μ g of vacuoles from BY4742 (1 and 2) or *vam10Δ* (3–5), with reaction buffer (10 mM Pipes-KOH, pH 6.8/200 mM sorbitol/40 mM KCl/0.1 mM $MgCl_2$ /10 μ M CoA/0.3 mM ATP/6 mM creatine phosphate/10 units/ml creatine kinase/7.5 ng/ml leupeptin/37.5 ng/ml pepstatin/3.75 μ M o-phenanthroline/7.5 μ M Pefabloc SC). After 25 min at 27°C, samples were chilled and stained with 5 μ M FM4–64 for 2 min. Half of each sample was mixed with 15 μ l of 0.7% low-melt agarose in PS buffer (10 mM Pipes-KOH, pH 6.8/200 mM sorbitol). Aliquots (15 μ l) were transferred to prechilled slides and cover slips. After 5 min at 4°C, samples were observed by fluorescence microscopy (five fields recorded per condition). (B) Contacts per vacuole in the focal plane was determined for 80–120 vacuoles for each condition in A.

Vacuole fusion (Fig. 5C, lane 3) was stimulated by Vam10p (lane 4) on the normal fusion pathway as it was inhibited by anti-Sec18p (lane 5). A two-step incubation was begun with anti-Sec18p for 20 min followed by recombinant Sec18p. Vam10p stimulation was seen only when Vam10p was present from the start of the reaction (lanes 6–8), even when ATP was omitted from the first incubation (lanes 9–11).

To show that Vam10p can act before Sec18p, a two-step reaction was used, exploiting Sec18p reversal of anti-Sec18p inhibition (3) and the capacity of anti-Vam10p to block the stimulation of fusion by Vam10p (Fig. 5D, lanes 5 and 6). When vacuoles first are incubated with Vam10p in the presence of anti-Sec18p and then mixed with sufficient antibody to Vam10p to block stimulation of fusion and given Sec18p, full fusion activity is seen (lanes 7 and 8). Accordingly, vacuoles from a *vam10Δ* strain show normal release of Sec17p (Fig. 5E). Vam10p is the first vacuole fusion factor that can act upstream of Sec18p, although our data do not address whether it must act upstream of Sec18p.

Vacuole priming is a prerequisite for tethering, the first association between vacuoles. Tethering (Fig. 6A, 1) is abolished by Gdi1p (Fig. 6A, 2), which extracts Ypt7p (20). Strikingly,

vam10Δ vacuoles do not tether (Fig. 6A, 3) unless pure Vam10p is added (Fig. 6A, 4). Vam10p-mediated tethering of *vam10Δ* vacuoles is still fully sensitive to Gdi1p (Fig. 6A, 5). Quantitation of the intervacuole contacts in multiple image fields (Fig. 6B) confirms the visual impressions. Thus, Vam10p is an ATP-independent priming factor, not coupled to Sec18p action or Sec17p release, which supports subsequent vacuole tethering.

Discussion

Vam10p is needed for vacuole fusion *in vivo* and *in vitro*. The *VAM10* gene lies within *VPS5*, yet it has a distinct function (Fig. 3). *VAM10* deletion does not lower vacuolar CPY (Fig. 4C) and thus is not a *VPS* gene. The *in vivo* role of Vam10p was confirmed by its being required for osmotic stress-induced fusion and by the vacuole fragmentation induced by Vam10p overexpression. *In vitro*, we find that Vam10p stimulates vacuole fusion, and antibody to Vam10p blocks fusion during priming. Vam10p has no detectable effect on Sec17p release, suggesting that it affects another early process. This is likely a new function, as the known events of priming all require ATP, whereas Vam10p can act before ATP addition. However, the strongly enhanced vacuolar levels of peripheral membrane proteins such as Sec18p, HOPS, and actin in the absence of Vam10p suggests that Vam10p might function in a release stage of their normal cycling between the vacuole and cytoplasm. Vam10p has no obvious homologs, in yeast or in other sequenced organisms, although it is in a cluster of trafficking genes between *ALG8* and *GYP1*. Because each aspect of vacuole fusion is conserved functionally in other membrane-fusion events (2), Vam10p may have functional, if not sequence, homologs in other fusion reactions.

The stages of priming that are needed for tethering are complex. Tethering needs neither Vam3p nor Vam7p, and the Ypt7p on tethered vacuoles is enriched in vertex rings (8). Ligands to ergosterol (22) and phosphoinositides (4) can inhibit during priming, and these lipids might have a role in establishing the vertex ring of Ypt7p in conjunction with Vam10p. The striking effect of Vam10p on the levels of vacuolar HOPS, Sec18p, and actin is in accord with their roles in early steps of the fusion pathway. (i) Vps41p, a subunit of the HOPS complex, has altered mobility and abundance in the absence of Vam10p (Fig. 4C); because both Ypt7p and Vam10p are needed for tethering, and HOPS is a Ypt7p-effector complex (23), this may reflect the functional role of Vam10p. (ii) Vacuoles from *vam10Δ* strains bear more Sec18p (Fig. 4C), suggesting a connection between these two priming factors. (iii) Actin disassembly, which is sensitive to jasplakinolide, is needed for an early docking stage of the reaction, because jasplakinolide allows Ypt7p-dependent tethering (14) but fusion becomes jasplakinolide-resistant sometime between Ypt7p action and the completion of docking (14). Our working model is that Vam10p participates in tethering along with Ypt7p, regulating crucial vacuole-bound proteins. Other functions for Vam10p could be to regulate phosphoinositide synthesis or turnover; to control the essential vacuolar gradients of protons, calcium, or other ions that are established *in vitro* during priming; or to interact with Vtc complex (24), SNARE complex, Ypt7p, actin, or other vacuolar proteins that act during priming and tethering.

We thank Drs. Charles Barlowe, Scott Emr, and Stefan Otte for discussions and Dr. Michael Snyder for strains. This work was supported by grants from the National Institute of General Medical Sciences, the Human Frontier Science Program Organization, and the Yokoyama Foundation for Clinical Pharmacology.

1. Rizo, J. & Sudhof, T. (2002) *Nat. Rev. Neurosci.* **3**, 641–653.
2. Wickner, W. (2002) *EMBO J.* **21**, 1241–1247.
3. Mayer, A., Wickner, W. & Haas, A. (1996) *Cell* **85**, 83–94.
4. Mayer, A., Scheglmann, D., Dove, S., Glatz, A., Wickner, W. & Haas, A. (2000) *Mol. Biol. Cell* **11**, 807–817.
5. Veit, M., Laage, R., Dietrich, L., Wang, L. & Ungermann, C. (2001) *EMBO J.* **20**, 3145–3155.

6. Mayer, A. & Wickner, W. (1997) *J. Cell Biol.* **136**, 307–317.
7. Wang, L., Seeley, S., Wickner, W. & Merz, A. (2002) *Cell* **108**, 357–369.
8. Wang, L., Merz, A. J., Collins, K. M. & Wickner, W. (2003) *J. Cell Biol.* **160**, 365–374.
9. Peters, C. & Mayer, A. (1998) *Nature* **396**, 575–580.
10. Seeley, E. S., Kato, M., Margolis, N., Wickner, W. & Eitzen, G. (2002) *Mol. Biol. Cell* **13**, 782–794.

11. Wada, Y., Ohsumi, Y. & Anraku, Y. (1992) *J. Biol. Chem.* **267**, 18665–18670.
12. Haas, A., Conradt, B. & Wickner, W. (1994) *J. Cell Biol.* **126**, 87–97.
13. Zhu, H., Bilgin, M., Bangham, R., Hall, D., Casamayor, A., Bertone, P., Lan, N., Jansen, R., Bidlingmaier, S., Houfek, T., *et al.* (2001) *Science* **293**, 2101–2105.
14. Eitzen, G., Wang, L., Thorngren, N. & Wickner, W. (2002) *J. Cell Biol.* **158**, 669–679.
15. Vida, T. A. & Emr, S. D. (1995) *J. Cell Biol.* **128**, 779–792.
16. Bone, N., Millar, J. B. A., Toda, T. & Armstrong, J. (1998) *Curr. Biol.* **8**, 135–144.
17. Ungermann, C., Wickner, W. & Xu, Z. (1999) *Proc. Natl. Acad. Sci. USA* **96**, 11194–11199.
18. Harlow, E. & Lane, D. (1988) *Antibodies: A Laboratory Manual* (Cold Spring Harbor Lab. Press, Plainview, NY).
19. Nothwehr, S. F. & Hines, A. E. (1997) *J. Cell Sci.* **110**, 1063–1072.
20. Horazdovsky, B. F., Davies, B. A., Seaman, M. N. J., McLaughlin, A., Yoon, S.-H. & Emr, S. D. (1997) *Mol. Biol. Cell* **8**, 1529–1541.
21. Haas, A., Scheglmann, D., Lazar, T., Gallwitz, D. & Wickner, W. (1995) *EMBO J.* **14**, 5258–5270.
22. Kato, M. & Wickner, W. (2001) *EMBO J.* **20**, 2035–2040.
23. Seals, D., Eitzen, G., Margolis, N., Wickner, W. & Price, A. (2000) *Proc. Natl. Acad. Sci. USA* **97**, 9402–9407.
24. Muller, O., Bayer, M. J., Peters, C., Andersen, J. S., Mann, M. & Mayer, A. (2002) *EMBO J.* **21**, 259–269.